# Automatic Bicycle Balance Assistance Reduces Probability of Falling at Low Speeds When Subjected to Handlebar Perturbations Version 1

Marten T. Haitjema Leila Alizadehsaravi Jason K. Moore

September 16, 2024

**Abstract**

Uncontrolled bicycles are generally unstable at low speeds. We add a controlled steering motor to a consumer electric bicycle that stabilizes it at low speeds. To test the motor's assistance during falls, we apply varying magnitude external handlebar perturbations to the bicycle while ridden on a treadmill with the balance assist system activated and deactivated. The probability of not recovering from a handlebar perturbation decreases when the balance assist is activated at a travel speed of 6 $\mathrm{km\,h^{-1}}$. Use of a balance assist system in real world bicycling will reduce the number of falls that occur near riders' control authority limits.

## 1 Introduction

Single-actor bicycle crashes are associated with a surprisingly large percentage of reported serious injuries (Wegman and Schepers, 2024). At low speeds, from start up to typical cruising speeds, bicycles themselves are not self-stable and can be challenging for the rider to balance. Low speed crashes may be reduced if the bicycle was self-stable at these speeds by relieving the rider of some of the necessary control activity. Bicycles can be mechanically modified to lower the speeds at which they are self-stable (Åström, Klein, and Lennartsson, 2005) and since the 1980s it has been known that applying a motor actuated steering torque proportional to the vehicle's roll rate can stabilize a single-track vehicle at lower speeds. If automatic control of steering can stabilize a bicycle, it may reduce the control required from the rider to successfully manage balancing tasks much like the high speed self-stability already does. We have developed a balance assisting bicycle, Figure 1, based on these principles and hypothesize that it helps the rider in situations in which they are likely to fall.

Riders fall when their control authority is not able to maintain a stable vehicle state. There are many real world scenarios that can put the vehicle into an uncontrollable state. External forces applied to the vehicle or rider are one such scenario type and natural examples include wind gusts, handlebars colliding with a neighbor's, a bag swinging from the handlebar, or simply hitting a bump in the road. To assess our balance assisting bicycle, we subject the rider to perturbations at the handlebar, which can relatively easily cause a rider to fall.

In this paper, we test whether a steer motor controlled bicycle, that is stable in a large low speed range, is beneficial in helping to prevent the rider from falling. We test this by applying varying magnitude mechanical perturbations to the handlebars while the rider is cycling on a treadmill. We assess the difference in the rider's probability of falling with the balance assist system on and off.

### 1.1 Technical Background

During the early years of developments in automatic control, (Whipple, 1899) not only derived the correct equations of motion of the bicycle but realized and showed that roll motion feedback can stabilize a bicycle. Much later, attempts at automatic roll stabilization of single-track vehicles began in earnest after predictive motorcycle models were developed and refined in throughout the 1970s. Van Zytveld (1975) was influenced by Whipple's work and seems to be the first to attempt to robotically stabilize a small motorbike with a controlled inverted pendulum that mimicked rider lean, but he was not successful in demonstrating what his theoretic control model correctly predicted. In his model, he recognized that


Figure 1: Balance assist bicycle prototype with electric motor in the steering column and data acquisition and control electronics mounted in the rear rack.

feedback of the vehicle roll angle and angular rate was essential to stabilize the vehicle. It was not until the early 1980s that Nagai, 1983 successfully demonstrated balancing a robotic bicycle on a treadmill with both steering control and a laterally moving mass. Ruijs and Pacjecka followed this by demonstrating an automatically balanced motorcycle (Ruijs and Pacejka, 1986) and they did so solely with a steering motor. Ruijs and Pacejka clearly showed that steer torque driven by roll angle feedback stabilizes the capsize mode, roll angular rate feedback stabilizes the weave mode, and steer angular rate feedback stabilizes the wobble mode. They also proposed how the gains must change with respect to vehicle speed for favorable control at all speeds. This roll motion feedback enables the simplest controller that can stabilize a single-track vehicle above a minimum speed when one is not concerned with wobble instabilities. Ruijs and Pacejka's work was not particularly concerned with low speed stability and their vehicle was fully automatic, i.e no human rider was involved.

Many more automatically balanced single track vehicles have been demonstrated over the last 40 years, but none have demonstrated that increasing low speed stability can assist in balancing and possibly reduce single-actor falls. Most of these robotic bicycle and motorcycle designers did not intend for a human rider to also control the stabilized vehicle. Nevertheless, an automatically stabilized bicycle can be controlled by a human rider if the motor controlled steer torque and the rider applied steer torque act on the steer in parallel. The effect of this automatic control gives the ability to effectively change the dynamics, up to some limits, of the human-controlled plant. In our prior study (Alizadehsaravi and Moore, 2023), we demonstrate reduced motion during distractions due to the balance assist system but contrarily researchers with a similar vehicle recently showed rider dissatisfaction with the stabilization Hanakam, Wehner, and Wrede, 2023.

The linear Carvallo-Whipple bicycle model (Carvallo, 1899; Whipple, 1899) is the simplest bicycle model that exhibits non-minimum phase behavior and self-stability. The bicycle model is suitable for showing the effect of a roll motion feedback driven steer motor on the dynamics. The linear version of this model (Meijaard et al., 2007) can be described by the fourth order state space equations:

$$\dot{\vec{x}} = \mathbf{A}\vec{x} + \mathbf{B}\vec{u} \text{ where } \vec{x} = \begin{bmatrix} \phi \\ \dot{\phi} \\ \delta \\ \dot{\delta} \end{bmatrix} \text{ and } \vec{u} = \begin{bmatrix} T_\phi \\ T_\delta \end{bmatrix}. \tag{1}$$

The states are the roll angle $\phi$ and steer angle $\delta$ along with their derivatives and the inputs are roll torque $T_\phi$ and steer torque $T_\delta$. The state $\mathbf{A}$ matrix is a function of the equilibrium forward speed $v$. It and the input $\mathbf{B}$ matrix are otherwise populated with expressions that are functions of the geometric and inertial parameters of the nonholonomic multibody system made up of four rigid bodies: two wheels, front frame, and rear frame.

If the steer torque is the sum of the (h)uman applied torque and the (m)otor applied torque $T_\delta$ =

$T_\delta^{\mathrm{h}} + T_\delta^{\mathrm{m}}$, $\mathbf{B} = \begin{bmatrix} \vec{B}_\phi & \vec{B}_\delta \end{bmatrix}$, and $T_\delta^{\mathrm{m}} = -k_{\dot{\phi}}\dot{\phi}$ then the human controlled plant takes the form:

$$\dot{\vec{x}} = \left( \mathbf{A} - \vec{B}_\delta \begin{bmatrix} 0 & k_{\dot{\phi}} & 0 & 0 \end{bmatrix} \right) \vec{x} + \mathbf{B} \begin{bmatrix} T_\phi \\ T_\delta^{\mathrm{h}} \end{bmatrix} \tag{2}$$

The state matrix $\mathbf{A}$ being a function of the equilibrium speed $v$ means $k_{\dot{\phi}}$ can be selected such that the eigenvalues of $\left( \mathbf{A} - \vec{B}_\delta \begin{bmatrix} 0 & k_{\dot{\phi}} & 0 & 0 \end{bmatrix} \right)$ have negative real parts for $v_{min} < v < v_{\mathrm{capsize}}$ where $v_{min}$ is the lowest stable speed given $k_{\dot{\phi}}$ and $v_{\mathrm{capsize}}$ is the speed at which the uncontrolled bicycle's capsize mode goes unstable. With gain scheduling with respect to $v$, the speed range where the bicycle is stable can be maximized within any physical actuator magnitude and bandwidth limits. Schwab, Kooijman, and Meijaard (2008) elaborates on some of the possibilities in scheduling the gains for such a controller and shows that a linear scheduling with respect to speed can give satisfactory stability for a low speed range. We use this simple feedback principle as the basis for our balance assist controller.

# 2 Methods

## 2.1 Bicycle

We modified an electric bicycle (Grenoble Arroyo, Royal Dutch Gazelle, Dieren, The Netherlands) with a custom motor in the steering assembly capable of applying up to 7 N m of torque between the head tube and steer tube, see Figure 1. A custom motor controller converts the commanded torque to applied torque. We measure the speed of the rear wheel with an encoder (Magura XXX) and measure the body fixed roll rate of the bicycle with a MEMs rate gyroscope (BN0086, Sparkfun, Niwot, USA). The balance assist control algorithm is implemented on a microprocessor (Teensy, PJRC, USA) and data from all sensors is logged with a CAN bus (CanEdge2, CSS Electronics, Denmark) at at least 100 Hz.

## 2.2 Balance Assist Control

We use a forward speed $v$ gain scheduled proportional roll rate feedback controller to stabilize the bicycle. In the speed range tested, the commanded steer torque $T_\delta^{\mathrm{m}}$ from the steer motor follows the control law

$$T_\delta^{\mathrm{m}} = -k_{\dot{\phi}}\dot{\phi} = g(v_{stable} - v)\dot{\phi} \tag{3}$$

where $v_{\mathrm{stable}} = 4.7\ \mathrm{m\,s^{-1}}$ is approximately the average stable speed predicted from the open loop bicycle rigid-rider dynamics. We use $g = 8$ and $g = 10$ as gain values during the experiments. Scaling the proportional feedback gain linearly with respect to speed stabilizes the normally unstable weave mode of the bicycle down to 2.9 $\mathrm{km\,h^{-1}}$ for the riderless bicycle and 4.6 $\mathrm{km\,h^{-1}}$ for the ridden bicycle as shown in Figure 2.

## 2.3 Perturbations

We apply longitudinal forces to the ends of each handlebar from Earth fixed posts using an adapted Bump'Em system (Tan, Raitor, and Collins, 2020) which we arrange with four motors working in cooperation, Figure 3b. The four motors are programmed to apply a light force at all times to keep the ropes taught and to track a commanded force profile using a PID controller running on a microprocessor (Arduino Mega 2560, Arduino, Italy). We measure the force applied by each motor at the handlebar via four inline 250 N S-style load cells except the left rear load cell that has a max load of 500 N. The commanded force profiles are designed to apply an external pulsive torque to the front assembly (handlebars, forks, wheel) at magnitudes varying from 16 N m to 160 N m. The four motors (EC-90 Flat, Maxon Group, Switzerland) are arranged at the four corners of a 1 m wide treadmill that can reach speeds of 18 $\mathrm{km\,h^{-1}}$. The general base design of this system is described in detail in Van De Velde's MSc thesis (van de Velde, 2022) and the physical arrangement is shown in Figure 3a. Our modifications relative to Van De Velde include simplifying the controller with a inexpensive microcontroller and the use of a simpler non-active safety harness.

## 2.4 Protocol

We recruited 26 able-bodied young adults (20-36 years old) to participate in the experiments. The subjects were all confident in their cycling skills and had cycled at least once in the last month. Eleven subjects

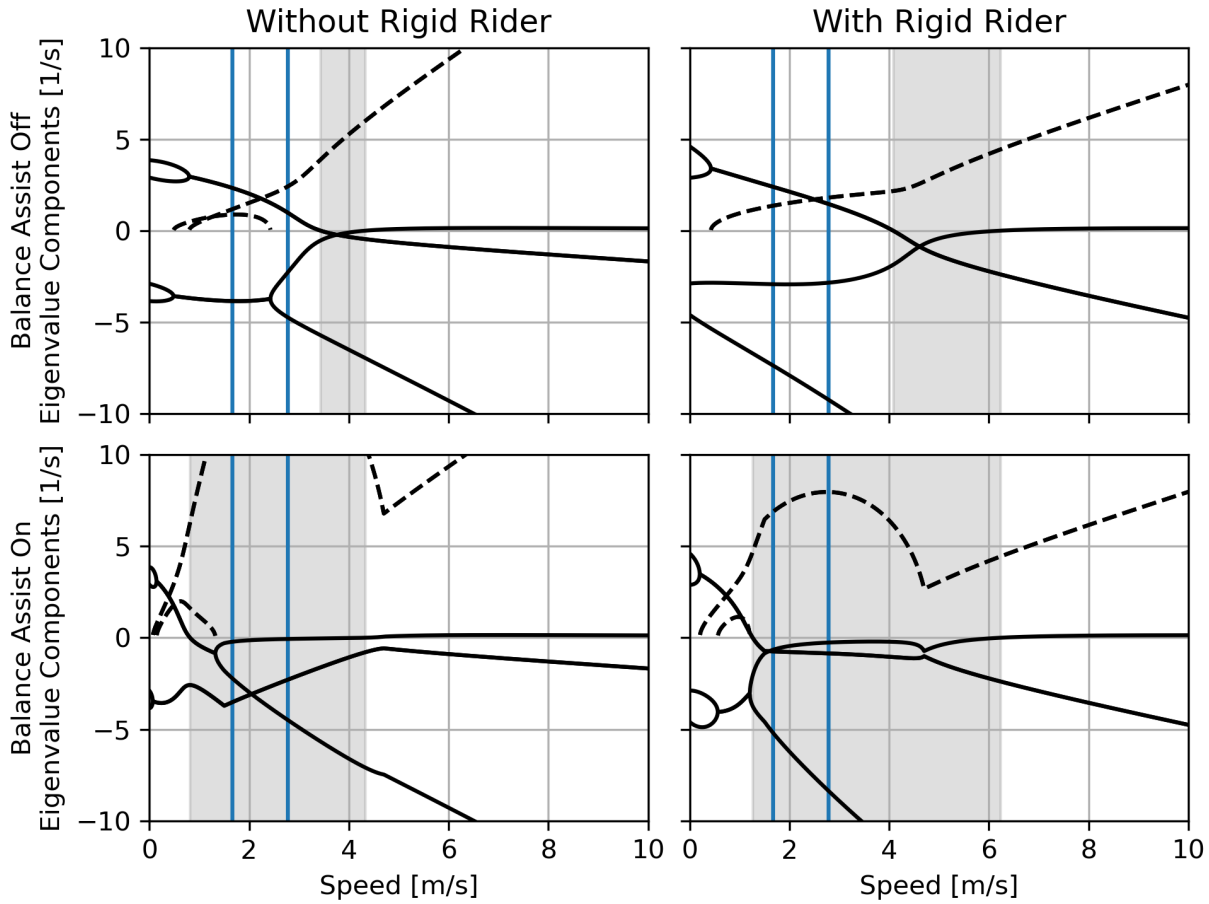


Figure 2: Uncontrolled (upper row) and controlled (lower row) root locus of eigenvalue components (real: solid, imaginary: dashed) plotted versus speed for the bicycle without the inertial effect of a rigid rider (left) and with a rigid rider (right). Vertical blue lines indicate the two speeds we perform experiments at. Grey shaded region is the linear stable speed range. Geometric and inertial parameters for these plots were estimated with the methods presented in Moore, 2012 and software packages BicycleParameters 1.1.1 (Moore et al., 2024) and Yeadon 1.5.0 (Dembia, Moore, and Hubbard, 2015).

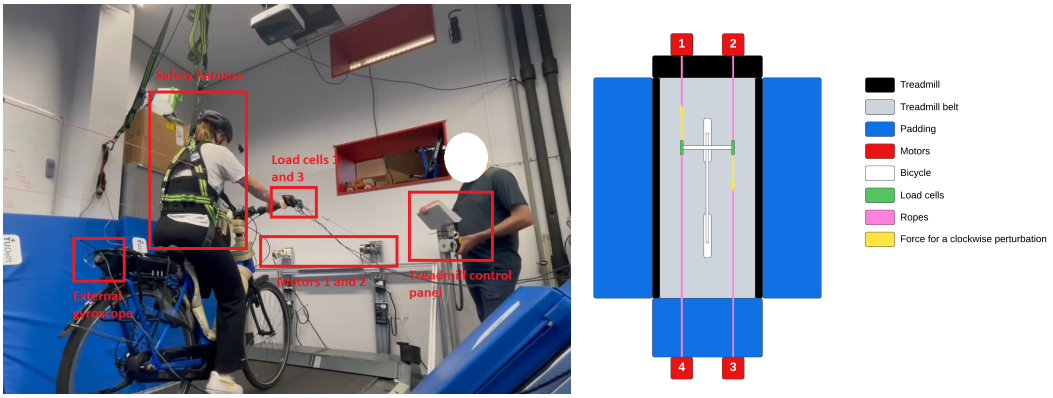


(a) A participant on the bicycle in the safety harness with the Bump'Em motor lines attached to the ends of the handlebars.

(b) Top view diagram of bicycle handlebar perturbation system.

Figure 3: Diagrams showing the Bump'Em system arranged to apply handlebar perturbations.

performed the experiments at 6 $\mathrm{km\,h^{-1}}$ (1.7 $\mathrm{m\,s^{-1}}$) and fifteen subjects performed the experiments at 10 $\mathrm{km\,h^{-1}}$ (2.8 $\mathrm{m\,s^{-1}}$). All subjects consented to the experiment and could decline to continue at any time. The study was approved by Delft University of Technology's Human Research Ethics Council (#3897).

The subjects were divided into two groups. The first group performed the protocol at a belt speed of 10 $\mathrm{km\,h^{-1}}$ with the controller gain set to $g = 8$ and the second group performed the protocol at a belt speed of 6 $\mathrm{km\,h^{-1}}$ with the controller gain set to $g = 10$. The 10 $\mathrm{km\,h^{-1}}$ group's experiments occurred two weeks before the 6 $\mathrm{km\,h^{-1}}$ group.

Subjects wore a helmet and fall safety harness attached to the ceiling Figure 3a. We allowed them to practice riding on the treadmill until they indicated they were comfortable enough to have perturbations applied. For most, this was less than a 10 min warm up. We then asked the rider to ride for 90 s, while attempting to maintain the location of their front wheel on the center line of the treadmill. We define a "fall" on the treadmill by two criteria: 1) the rider removes their foot from the pedal and places it on the ground or 2) the bicycle wheel exceeds the width of the treadmill belt. We then applied perturbations in random directions (clockwise or counter-clockwise), starting at 20 N and increasing the magnitude by 30 N until the participants fell. Figure 4 shows an example resulting motion from a perturbation. We log the magnitude that causes the first fall to characterize that subject's *nominal fall threshold*.

Following the initial threshold determination, we choose perturbation forces according to a random and adaptive staircase procedure applying perturbations above and below the initial perturbation threshold, while allowing small progression of the perturbation threshold to accommodate learning effects. Five possible perturbation forces are determined based on the initial perturbation threshold estimate: the initial estimate itself, two perturbations lower than the initial estimate, and two perturbations higher than the initial estimate. The five possible perturbations are separated by 10 N steps. For example, if the initial estimate of the perturbation threshold of a participant is 80 N, the five possible perturbations are 60, 70, 80, 90 and 100 N. Which one of these five perturbations is chosen is determined at random. If the perturbation results in a fall, the estimate of the perturbation threshold is decreased by 10 N, and vice versa if the perturbation did not result in a fall. Five new possible perturbation forces are determined around the updated perturbation threshold, and a new perturbation is selected at random. This process iterates until twenty perturbations are applied. The goal of this adaptive staircase procedure is to have participants fall for approximately 50% of the time. After the first set of 20 perturbations, we let the cyclist rest and then perform another 20 perturbations. We randomize whether the balance assist system is on or off during the first or second set of perturbations for each participant.

## 2.5 Measurements

We measure the time histories of the Bump'Em delivered perturbation forces and the bicycle's steer angle, roll angle, roll angular rate, and forward speed. Figure 5 shows an example perturbation force measurement compared to our Bump'Em controller command.

Based on findings from measuring riders without balance assist Haitjema, 2023, we calculate several variables that we hypothesize may influence fall probability. We use the angular impulse $L$ of the perturbation forces over a 0.3 s duration to characterize the magnitude of delivered perturbation. The duration is selected based on the duration of the commanded force and is calculated as follows:

$$L = \int_{0\mathrm{s}}^{0.3\mathrm{s}} \frac{l}{2}(F_r + F_l)dt = \int_{0\mathrm{s}}^{0.3\mathrm{s}} \frac{l}{2}\left[(F_{rf} - F_{rr}) + (F_{lf} - F_{lr})\right] dt. \tag{4}$$

where $F_r$ and $F_l$ is the total force applied on the right and left handlebar ends, respectively which are the sum of the rear and front load cell readings $F_{rr}$ and $F_{rf}$, for example. The handlebar length is given as $l$ in Equation 4.

At the initiation of each perturbation we log the instantaneous steer and roll angles to characterize the configuration of the bicycle when perturbed. The gain setting on the balance assist controller indicates if the assistance is off $g = 0$ or on at two different levels: low $g = 8$ or high $g = 10$. A recovery from the perturbation is successful if the person neither places their foot down onto the treadmill surface or their wheel of the bicycle exits the width of the treadmill belt. We record this as a binary variable $f$ for "fall". All measured variables are reported in Table 1.

## 2.6 Statistics

We test our hypothesis that the balance assistance controller will reduce the probability of falling when perturbed externally at the handlebar. We have a single binary fall outcome variable $f$ that is dependent

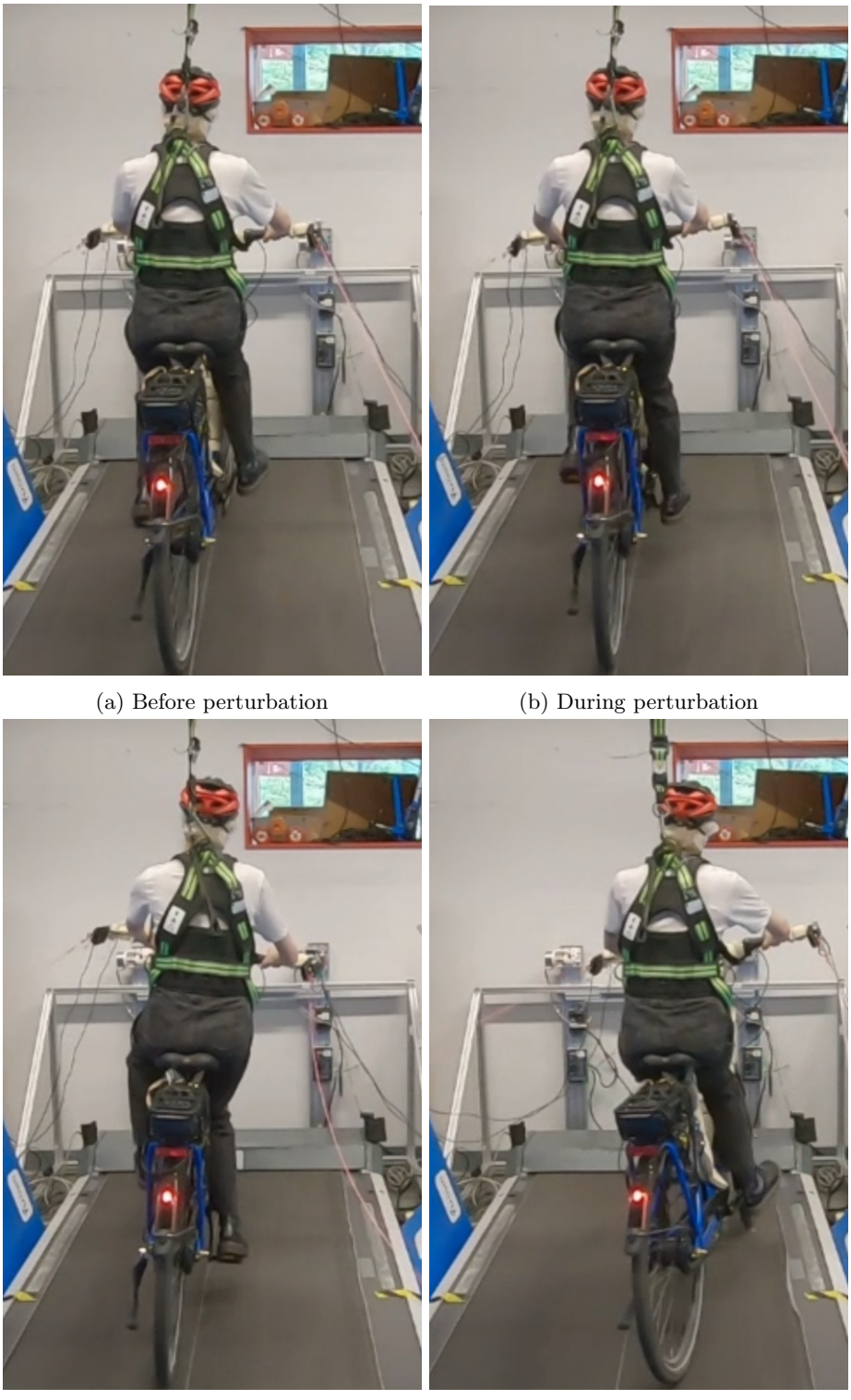

(a) Before perturbation (b) During perturbation

(c) After perturbation (d) Recovery from perturbation

Figure 4: Video frames depicting the application of a perturbation and the rider's response and recovery.

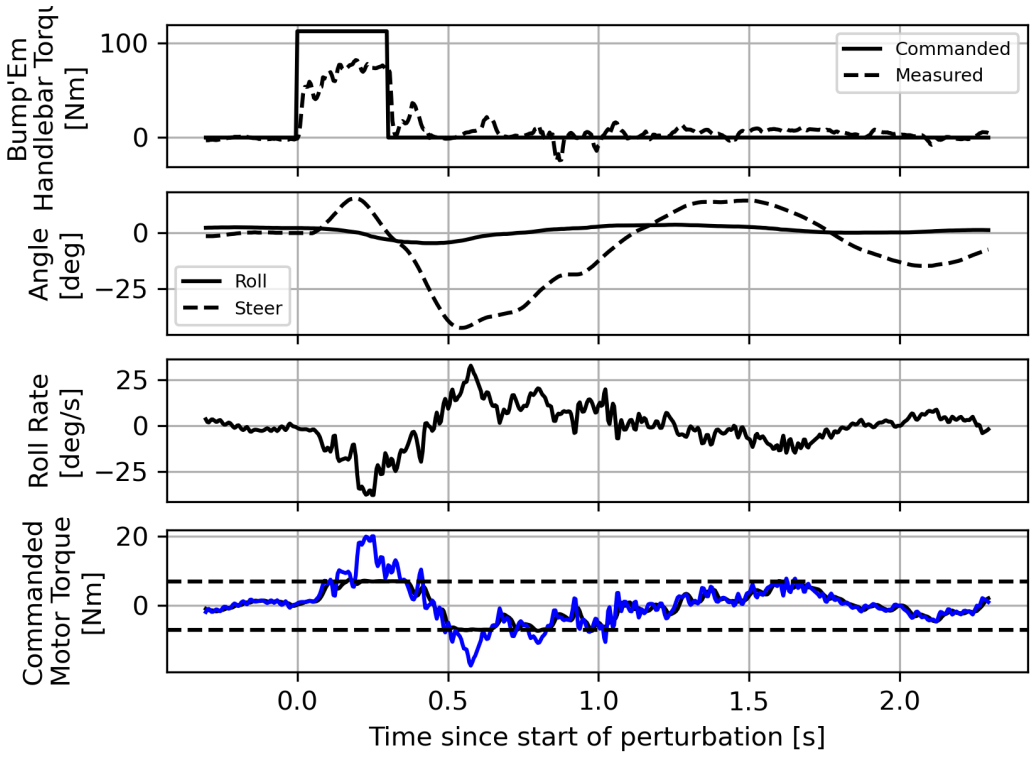


Figure 5: Motor force and resulting steer torque perturbation based on an 110N counterclockwise applied force.

Table 1: Raw measurements taken during each trial. "Fall outcome" and "Perturbation order number" are recorded per perturbation instance. The remaining measures are time varying during each trial.

| Measure | Variable | Units | Sensor |
|---|---|---|---|
| Balance Assist Gain | $g$ | $\mathrm{N\,s^2}$ | NA |
| Bicycle Speed | $v$ | $\mathrm{m\,s^{-1}}$ | wheel encoder |
| Fall outcome | $f$ | boolean | NA |
| Force $left/right, front/rear$ | $F_{lf}, F_{rf}, F_{lr}, F_{rr}$ | N | inline load cell |
| Perturbation Order Number | $j$ | integer | NA |
| Roll Angle | $\phi$ | $^\circ$ | BN0086 Kalman estimate |
| Roll Angular Rate | $\dot{\phi}$ | $^\circ\,\mathrm{s^{-1}}$ | BN0086 rate gyroscope |
| Steer Angle | $\delta$ | $^\circ$ | steer tube encoder |

Table 2: Independent and dependent variables used in the statistical model.

| Variable | Causality | Units | Description |
|---|---|---|---|
| $L$ | independent | N m s | angular impulse of perturbation torque |
| $\delta_0$ | independent | ° | steer angle at start of perturbation |
| $\phi_0$ | independent | ° | roll angle at start of perturbation |
| $f$ | dependent | boolean | outcome: did not fall 0 or did fall 1 |
| $c$ | independent | boolean | balance assist: off 0 or on 1 |
| $j$ | independent | integer | order number of perturbation |

on several possible explanatory independent variables, one of which is the binary balance assistance (on or off). See Table 2 for the statistical model variables.

We evaluate this hypothesis using a multivariate logistic regression model that takes the general form

$$f_{ij}|p_{ij} \sim \text{Bern}(p_{ij}). \tag{5}$$

Fall outcome $f_{ij}$ is the binary outcome of perturbation $j$ on participant $i$ which follows a Bernoulli distribution given the probability $p_{ij}$ that a fall occurs. The log-odds of the probability is then a linear function of our independent variables with $\beta$ being the intercept and $\alpha_k$ the linear coefficients to the $K$ independent variables $x_{ij}^k$, i.e. all variables in Table 2 except $f$.

$$\log\left(\frac{p_{ij}}{1-p_{ij}}\right) = \beta + \sum_{k=0}^{K} \alpha_k x_{ij}^k \tag{6}$$

Before fitting the model, we scale each independent variable $x_{ij}^k$ such that they have a mean of zero and a standard deviation of one by cluster-mean centering, as recommended by Enders and Tofighi, 2007, with clusters being an individual subject. The clusters are chosen as all data from an individual subject because we are only interested in the association between the state of the balance-assist system and the outcome of the perturbation. We expected there to be a variation between participants in how well they are able to resist the perturbation. However, this was not true. Cluster-mean centering shows there to be no variation between participants. This fact allows us to utilize a simple single-level logistic regression model, instead of a multilevel model. This left us with angular impulse, perturbation order, balance assist state, and roll & steer angles at the time of perturbation as independent variables. We also include interaction effects between the balance assist state and the other four variables. We divide the analysis into two separate model evaluations, one for the 6 km h$^{-1}$, $g = 10$ trials and one for the 10 km h$^{-1}$, $g = 8$ trials and we evaluate our hypothesis for each set of data.

# 3 Results

The coefficient estimates for a single-level logistic regression for the data from the 6 km h$^{-1}$, gain $g = 10$ trials are shown in Table 3. The angular impulse, perturbation order, and balance assist state are all statistically significant predictors with angular impulse having a dominant effect. Larger angular impulse increases the probability to fall and enduring more perturbations or having the balance assist on, decrease the probability to fall. The associated multiplicative change in odds are shown in Table 3.

The coefficient estimates for a single-level logistic regression at 10 km h$^{-1}$ with gain $g = 8$ are shown in Table 4. The angular impulse and perturbation order are statistically significant predictors with angular impulse being the dominant effect. Larger angular impulse increases the probability to fall and enduring more perturbations decreases the probability to fall. Unlike the 6 km h$^{-1}$ trials, the balance assist state is not a significant predictor. At both speeds the angular impulse has about twice the effect as the perturbation order.

Turning the balance-assist system on significantly ($p < 0.05$) reduces the odds that a perturbation results in a fall while cycling at a speed of 6 km h$^{-1}$. Figure 6a visualizes the probability of falling as a function of the mean and centered angular impulse per participant for the balance assist state on and off while keeping all other explanatory factors at their centered mean values. This figure is created by setting all explanatory variables to there mean and calculating the probability from Eq 6 for only change in angular impulse given the estimates in Table 3. The table indicates that the balance-assist system

Table 3: Logistic regression coefficient estimates $\alpha_k$ at 6 $\mathrm{km\,h^{-1}}$ and gain $g = 10$ along with the standard error SE, p-value $p$, multiplicative change in odds $e^{\alpha_k}$, and the 5% confidence interval bounds.

| Variable | $\alpha_k$ | SE | $p$ | $e^{\alpha_k}$ | 2.5% | 97.5% |
|---|---|---|---|---|---|---|
| Intercept $\beta$ | -0.29 | 0.17 | 0.09 | 0.75 | 0.53 | 1.05 |
| Angular impulse $L$ | 1.69 | 0.27 | 0.00* | 5.40 | 3.18 | 9.16 |
| Perturbation order $j$ | -0.77 | 0.22 | 0.00* | 0.46 | 0.30 | 0.72 |
| Balance assist state $c$ | -0.64 | 0.27 | 0.02* | 0.53 | 0.31 | 0.89 |
| Roll angle $\phi_0$ | -0.25 | 0.21 | 0.24 | 0.78 | 0.51 | 1.18 |
| Steer angle $\delta_0$ | -0.14 | 0.21 | 0.51 | 0.87 | 0.58 | 1.32 |
| Balance assist state × roll angle | 0.52 | 0.34 | 0.12 | 1.68 | 0.86 | 3.29 |
| Balance assist state × steer angle | -0.41 | 0.34 | 0.22 | 0.66 | 0.34 | 1.28 |
| Balance assist state × angular impulse | 0.41 | 0.41 | 0.32 | 1.51 | 0.67 | 3.38 |
| Balance assist state × perturbation order | -0.53 | 0.34 | 0.12 | 0.59 | 0.30 | 1.15 |

Table 4: Logistic regression coefficient estimates $\alpha_k$ at 10 $\mathrm{km\,h^{-1}}$ and gain $g = 8$ along with the standard error SE, p-value $p$, multiplicative change in odds $e^{\alpha_k}$, and the 5% confidence interval bounds.

| Variable | $\alpha_k$ | SE | $p$ | $e^{\alpha_k}$ | 2.5% | 97.5% |
|---|---|---|---|---|---|---|
| Intercept | -0.24 | 0.16 | 0.13 | 0.78 | 0.57 | 1.07 |
| Angular impulse $L$ | 2.39 | 0.29 | 0.00* | 10.92 | 6.23 | 19.13 |
| Perturbation order $j$ | -1.16 | 0.21 | 0.00* | 0.31 | 0.21 | 0.48 |
| Balance-assist on $c$ | -0.44 | 0.24 | 0.07 | 0.64 | 0.40 | 1.03 |
| Roll angle $\phi_0$ | 0.27 | 0.22 | 0.22 | 1.31 | 0.85 | 2.04 |
| Steer angle $\delta_0$ | -0.37 | 0.24 | 0.12 | 0.69 | 0.43 | 1.10 |
| Balance assist state × roll angle | -0.61 | 0.34 | 0.08 | 0.54 | 0.28 | 1.07 |
| Balance assist state × steer angle | 0.56 | 0.35 | 0.11 | 1.76 | 0.88 | 3.50 |
| Balance assist state × angular impulse | 0.46 | 0.44 | 0.29 | 1.59 | 0.68 | 3.74 |
| Balance assist state × perturbation order | -0.37 | 0.32 | 0.25 | 0.69 | 0.37 | 1.30 |

halves (0.53) the odds that a perturbation results in a fall. This figure shows that for relatively large impulses the probability to fall is unity for both states of balance assist on and off. And for relatively small impulses the probability to fall is null for both states. But for impulses in the magnitude region (-1 to 0.5 STD), i.e. around the mean-centered fall threshold, the probability of falling is significantly lowered with the balance assist system on. The skewness of the probability curves arrives from the interaction effects. Figure 6b shows the same result for the 10 $\mathrm{km\,h^{-1}}$ trials which has a similar trend of reducing the probability to fall with the balance assist system turned on, but the effect is not significant.

# 4 Discussion

We have shown that at a 6 $\mathrm{km\,h^{-1}}$ riding speed the addition of balance assist control reduces the chance that a rider will fall when perturbed around the limits of their control authority. But this effect diminishes just below significance at the higher speed scenario of 10 $\mathrm{km\,h^{-1}}$. We were only able to test these two speed-gain scenarios for mostly homogeneous sets of riders within the resources of this research project, but additional experimental work could help understand more completely the range and limits of the positive effect of the balance system. For example, it is possible that simply increasing the controller gain at 10 $\mathrm{km\,h^{-1}}$ also results in a significant positive effect. A longitudinal study of normal use of the balance assist bicycle compared to a control group could provide the strongest evidence of any benefit we have seen in this more narrow scenario.

## 4.1 Stability and Human Controlled Plant Dynamics

The linear Carvallo-Whipple model indicates that the steer controller stabilizes the bicycle-rider system, but this model assumes the rider's hands are not connected to the handlebars and that they clamp their body as rigidly as possible to the rear frame. In reality, the system's behavior is likely more akin to a marginally stable or an easily controllable unstable system due to the various un-modeled effects. Our system may not result in a definitely stable system, i.e. cannot fall, but having plant eigenvalues with very small unstable eigenvalue real parts correlates to ease of control (Hess, Moore, and Hubbard, 2012).

The controller design we utilize, Equation 3, also increases the weave mode frequency by a factor of about three up to about 1 Hz. This bandwidth is still controllable by the human's neuromuscular system, but may feel unnatural as it is more akin to what the steering would feel like at in the 30 $\mathrm{km\,h^{-1}}$ to 40 $\mathrm{km\,h^{-1}}$ speed range. Hanakam, Wehner, and Wrede (2023) reported dissatisfaction in subjective rider feeling on their similar bicycle to ours and this effect to the human-controlled plant dynamics could be connected to this.

## 4.2 Application of the Logistic Model

The probability that a fall occurs depends on the values of all the independent variables in Table 2, but we can visualize the effect of one or two variables (e.g. Figure 6) to gain some insight. But to interpret the results in Tables 3 and 4 it is important to understand the relationship between probability and odds. The estimate in Table 3 shows that the balance assist system halves the odds that a perturbation results in a fall: $e^{\alpha_k} = 0.53$. This means if the odds are a 1000:1, turning on the balance-assist system reduces the odds to 500:1. However, that case the probability that a fall occurs is only reduced from 0.999 to 0.998. If the odds that a fall will occur are smaller, halving the odds has a larger influence on the fall probability. For example, if the odds that a fall occurs is two, halving it to one reduces the probability from 0.66 to 0.50. This can be seen in Figure 6 which shows the fall probability as a function of the magnitude of the normalized angular impulse for both speeds. The difference in probability between the balance-assist on/off case becomes insignificant outside of approximately $\pm 1$ standard deviation of the average angular impulse the rider was subjected to. This means that the balance assist is most effective for perturbations close to the subject's personal threshold between falling or recovery and that large perturbations will make you fall regardless of the balance assist's help.

To illustrate the effect of the balance-assist system on fall probability, we will give an example of how the data collected during the experiments is used to predict fall probability. We use Equation 6 and the coefficients in 3. For simplicity's sake, the interaction effects are not included. For example, assuming that the mean angular impulse $\bar{L}$ of all the perturbations applied to a participant is 100 N, and the standard deviation $\sigma^L = 15$. The centered and scaled angular impulse can be calculated by subtracting $\bar{L}$ from the applied angular impulse $L$, and dividing this by $\sigma^L$. The same applies for the perturbation order $j$, initial roll angle $\phi_0$, and initial steer angle $\delta_0$. If we take the coefficients estimated for cycling at

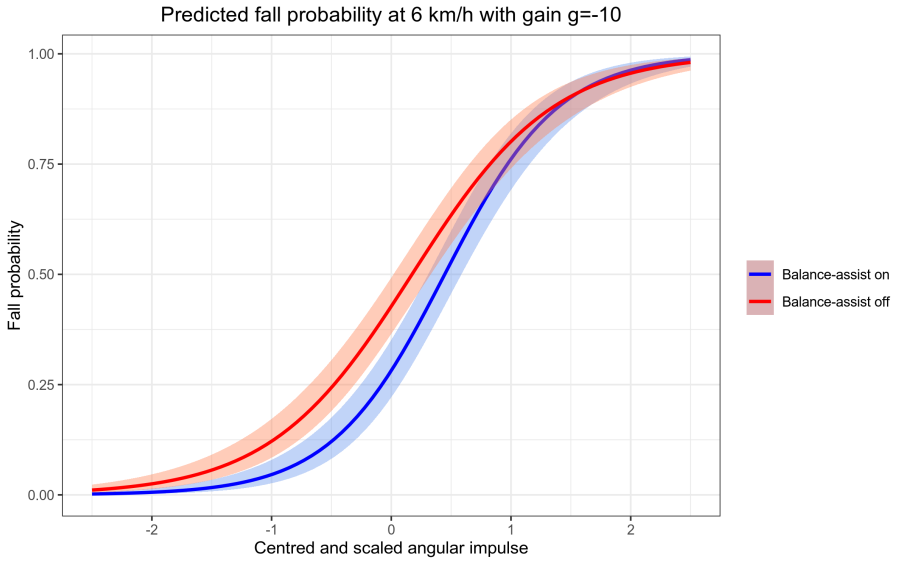


(a)

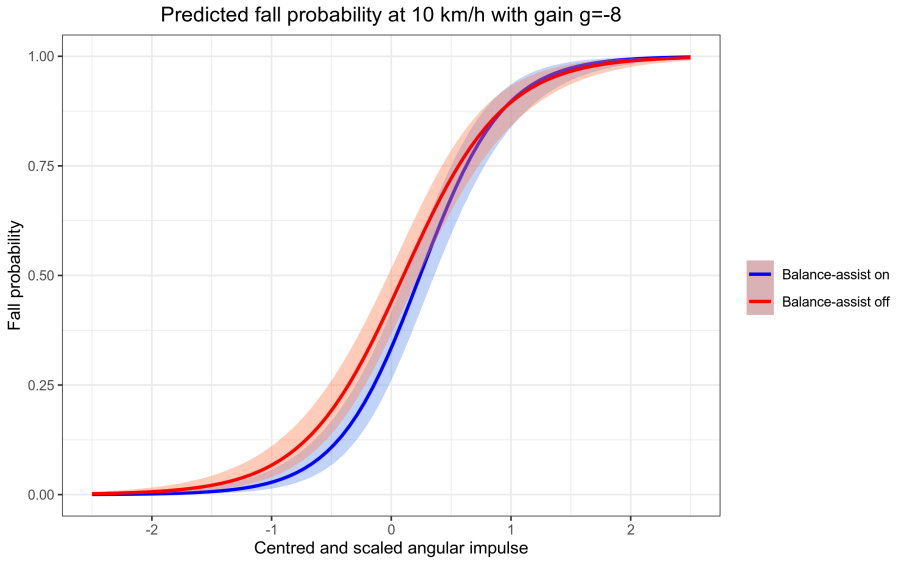


(b)

Figure 6: Comparison of predicted fall probability for balance-assist on (blue) or off (red) when all other predictor variables are fixed at zero, except for the interaction effect between the balance-assist and the angular impulse. The ordinate axis is standard deviation around the mean (all perturbations), centered per participant.

6 km h$^{-1}$, the log-odds of falling can be calculated as follows.

$$\begin{aligned}\log\left(\frac{p_{ij}}{1-p_{ij}}\right) = &\quad \beta + \sum_{k}^{k=0} \alpha_k \frac{x_{ij}^k - \bar{x_{ij}^k}}{\sigma^{x^k}} \\ &= -0.29 + 1.69 \cdot \frac{110\text{ N} - 115\text{N}}{15\text{N}} - 0.77 \cdot \frac{10-20}{11.54} \\ &\quad - 0.25 \cdot \frac{-6^\circ - 2^\circ}{10^\circ} - 0.14 \cdot \frac{1^\circ + 3^\circ}{5^\circ} - 0.64 \cdot c \\ &= 1.42 - 0.64 \cdot c\end{aligned} \tag{7}$$

The state of the balance-assist $s$ is a binary variable. If the balance-assist is turned on, the log-odds that a fall occurs are decreased by 0.64. The odds and probability can be calculated:

$$\frac{p_{ij}}{1-p_{ij}} = e^{1.42-0.64c} = e^{1.42} \cdot e^{-0.64s} = 4.14 \cdot 0.53c \tag{8}$$

$$p_{ij}|_{c=0} = \frac{4.14}{1+4.14} = 0.81 \tag{9}$$

$$p_{ij}|_{c=1} = \frac{4.14 \cdot 0.53}{1+4.14 \cdot 0.53} = 0.69 \tag{10}$$

Turning on the balance-assist system reduces the probability that the perturbation results in a fall from 81% to 69%.

This illustration alludes to the difficulty needed to apply the model in way that could predict how many falls may be averted in a natural setting if the balance assist system is used. Estimates of the predictor variables extracted from the limited data collected from natural cycling would be needed to populate the model.

## 4.3 Treadmill Width

Angular impulse magnitude has the largest significant effect for predicting fall probability as seen in both Tables 3 and 4. An increase in angular impulse increases the fall probability both at 6 and 10 km h$^{-1}$. At 10 km h$^{-1}$, the multiplicative change in odds is approximately twice as big as at 6 km h$^{-1}$. Thus, angular impulse is a more important predictor at higher speeds compared to lower speeds. We posit that this likely has to do with the width of the treadmill and that this could also be why the balance assist system did not have a statistically significant effect at 10 km h$^{-1}$. As a bicycle travels at higher speeds, the same perturbation magnitude causes larger lateral deviations. At 10 km h$^{-1}$ almost all falls were due to the bicycle exiting the maximum width of the treadmill. If the same experiment was performed on an infinitely wide plane, the riders may have recovered from more perturbations. At 6 km h$^{-1}$ the riders could often recover in the allotted treadmill width due to the smaller lateral deviations. We believe our results are very much dependent on the two modes of falling with use: exit the treadmill width or foot is placed on the belt. Cycle paths are a similar width as the treadmill, so rider's are often limited in width when recovering from a fall.

## 4.4 Learning Effect

An increase in the number of perturbation that a participant already experienced, decreases the probability that a fall occurs. This is likely due to the participants learning how to better recover from the perturbation over the duration of the experiment. This effect is significant at both 6 and 10 km h$^{-1}$, and in the same order of magnitude. This suggests that the learning effect that occurs during the experiment is not strongly dependent on the speed.

## 4.5 Non-significant Predictors

Roll and steer angle are not a significant predictor of fall probability at 6 or at 10 km h$^{-1}$. We expected these variables to have a significant effect based on the following reasoning. If you are in a rolled and steered state that is far from the upright equilibrium, then a perturbation that further pushes you from the equilibrium should have some additive or multiplicative effect on the resulting motion trajectory.

None of the interaction effects are statistically significant. That means that whether the balance-assist system is on or off does not significantly change the effect that the roll angle, steer angle, angular impulse, and perturbation order have on the probability that a fall will occur.

### 4.6 Extrapolation to Natural Falls

The positive effect of the balance assist system is coupled to the assumptions and experimental scenarios we implemented and there is unfortunately no simple way to extrapolate our results to reductions of single-actor crashes we may see if such a system were deployed widely to bicyclists. Although, our results do indicate that we would see such a reduction, even if only in a class of single-actor crashes that most resemble our experimental design. If there were more comprehensive and detailed natural data of how people fall we could make estimates on the number of falls reduced if everyone road a balance assist bicycle.

## 5 Conclusion

Automatically controlling a steering motor in a bicycle using roll rate feedback lowers the speed at which the bicycle is stable. This makes the bicycle's low speed dynamics more akin to its uncontrolled high speed dynamics, which is easier for a rider to balance. Perturbation forces applied to the handlebar can cause a rider to fall and every rider has a threshold force at which they are more likely to fall than not. The probability of falling when mechanically perturbed is significantly reduced when traveling at 6 $\mathrm{km\,h^{-1}}$ when the balance assisting control is activated. This effect is present when traveling at 10 $\mathrm{km\,h^{-1}}$ but more investigation is needed to determine if the effect can be significant. The positive effect to balance is rider independent and most effective in the regime of perturbations near the rider's control authority threshold. Given that similar effects cause falls during bicycling, use of the balance assist system in real world use cases will reduce the number of falls at low bicycling speeds.

## Acknowledgements

This study follows and draws from experimental and analysis methods originally developed in unpublished research by Marco Reijne. The authors acknowledge Felix Dauer, David Gabriel, Sierd Heida, Oliver Maier, Maarten Pelgrim, Marco Reijne, and Arend Schwab for contributions to the development of the balance assist bicycle.

## Funding

This study is funded by Dutch Research Council, Nederlandse Organisatie voor Wetenschappelijk Onderzoek (NWO), under the Citius Altius Sanius program and in collaboration with Bosch eBike Systems and Royal Dutch Gazelle. The funders had no role in the data collection and analysis or preparation of the manuscript.

## References

Alizadehsaravi, Leila and Jason K. Moore (Oct. 17, 2023). "Bicycle Balance Assist System Reduces Roll and Steering Motion for Young and Older Bicyclists during Real-Life Safety Challenges". In: *PeerJ* 11, e16206. ISSN: 2167-8359. DOI: 10.7717/peerj.16206.

Åström, Karl J., Richard E. Klein, and Anders Lennartsson (Aug. 22, 2005). "Bicycle Dynamics and Control: Adapted Bicycles for Education and Research". In: *IEEE Control Systems Magazine* 25.4, pp. 26–47. ISSN: 1066-033X, 1941-000X. DOI: 10.1109/MCS.2005.1499389.

Carvallo, E. (1899). *Théorie Du Mouvement Du Monocycle et de La Bicyclette*. Paris, France: Gauthier- Villars.

Dembia, Chris, Jason K. Moore, and Mont Hubbard (Apr. 7, 2015). "An Object Oriented Implementation of the Yeadon Human Inertia Model". In: *F1000Research* 3.233. DOI: 10.12688/f1000research.5292.2.

Enders, Craig K. and Davood Tofighi (2007). "Centering Predictor Variables in Cross-Sectional Multilevel Models: A New Look at an Old Issue". In: *Psychological Methods* 12.2, pp. 121–138. ISSN: 1939-1463. DOI: 10.1037/1082-989X.12.2.121.

Haitjema, Marten Tjeerd (Dec. 14, 2023). "Estimating Fall Probability in Cycling". MSc. Delft, The Netherlands: Delft University of Technology.

Hanakam, Yannick, Christa Wehner, and Jürgen Wrede (Jan. 3, 2023). "The Influence of an Active Steering Assistance System on the Cyclist's Experience in Low-Speed Riding Tasks". Poster. Interntional Cycling Safety Conference (Dresden, Germany).

Hess, Ronald, Jason K. Moore, and Mont Hubbard (Feb. 10, 2012). "Modeling the Manually Controlled Bicycle". In: *IEEE Transactions on Systems, Man, and Cybernetics - Part A: Systems and Humans* 42.3, pp. 545–557. ISSN: 1083-4427, 1558-2426. DOI: 10.1109/TSMCA.2011.2164244.

Meijaard, J. P. et al. (Aug. 2007). "Linearized Dynamics Equations for the Balance and Steer of a Bicycle: A Benchmark and Review". In: *Proceedings of the Royal Society A: Mathematical, Physical and Engineering Sciences* 463.2084, pp. 1955–1982. DOI: 10.1098/rspa.2007.1857.

Moore, Jason K. (Aug. 21, 2012). "Human Control of a Bicycle". Doctor of Philosophy. Davis, CA: University of California. 398 pp. URL: http://moorepants.github.io/dissertation.

Moore, Jason K. et al. (Apr. 26, 2024). *BicycleParameters: A Python Library for Bicycle Parameter Estimation and Analysis*. Version 1.1.1. URL: https://github.com/moorepants/BicycleParameters.

Nagai, M. (1983). "Analysis of Rider and Single-Track-Vehicle System; Its Application to Computer-Controlled Bicycles". In: *Automatica* 19.6, pp. 737–740.

Ruijs, P.A.J. and H.B. Pacejka (1986). "Recent Research in Lateral Dynamics of Motorcycles". In: *Vehicle System Dynamics* 15 (sup1), pp. 467–480. ISSN: 0042-3114. DOI: 10.1080/00423118608969155.

Schwab, A. L., J. D. G. Kooijman, and J. P. Meijaard (Sept. 8, 2008). "Some Recent Developments in Bicycle Dynamics and Control". In: Fourth European Conference on Structural Control (4ECSC). St. Petersburg, Russia, pp. 1–8.

Tan, Guan Rong, Michael Raitor, and Steven H. Collins (May 2020). "Bump'em: An Open-Source, Bump-Emulation System for Studying Human Balance and Gait". In: *2020 IEEE International Conference on Robotics and Automation (ICRA)*. 2020 IEEE International Conference on Robotics and Automation (ICRA), pp. 9093–9099. DOI: 10.1109/ICRA40945.2020.9197105.

Van de Velde, Shannon (Mar. 29, 2022). "Design of a Setup for Experimental Research on Stability of a Bicycle-Rider System Subject to Large Perturbations". MSc. Delft, The Netherlands: Delft University of Technology.

Van Zytveld, P. (1975). "A Method for the Automatic Stabilization of an Unmanned Bicycle". PhD thesis. Stanford University.

Wegman, Fred and Paul Schepers (Feb. 1, 2024). "Safe System Approach for Cyclists in the Netherlands: Towards Zero Fatalities and Serious Injuries?" In: *Accident Analysis & Prevention* 195, p. 107396. ISSN: 0001-4575. DOI: 10.1016/j.aap.2023.107396.

Whipple, Francis J. W. (1899). "The Stability of the Motion of a Bicycle". In: *Quarterly Journal of Pure and Applied Mathematics* 30, pp. 312–348.